



Order Parameters of a Transmembrane Helix in a Fluid Bilayer: Case Study of a WALP Peptide

Andrea Holt, Léa Rougier, Valérie Réat, Franck Jolibois, Olivier Saurel, Jerzy Czaplicki, J. Antoinette Killian, Alain Milon

► To cite this version:

Andrea Holt, Léa Rougier, Valérie Réat, Franck Jolibois, Olivier Saurel, et al.. Order Parameters of a Transmembrane Helix in a Fluid Bilayer: Case Study of a WALP Peptide. *Biophysical Journal*, 2010, 98 (9), pp.1864-1872. <10.1016/j.bpj.2010.01.016>. <hal-02322509>

HAL Id: hal-02322509

<https://hal.science/hal-02322509v1>

Submitted on 11 Apr 2023

HAL is a multi-disciplinary open access archive for the deposit and dissemination of scientific research documents, whether they are published or not. The documents may come from teaching and research institutions in France or abroad, or from public or private research centers.

L'archive ouverte pluridisciplinaire **HAL**, est destinée au dépôt et à la diffusion de documents scientifiques de niveau recherche, publiés ou non, émanant des établissements d'enseignement et de recherche français ou étrangers, des laboratoires publics ou privés.



HAL Authorization

Order parameters of a transmembrane helix in a fluid bilayer: case study of a WALP peptide.

Andrea Holt^{4#}, Léa Rougier^{1,2,3#}, Valérie Réat^{1,3}, Franck Jolibois^{2,3}, Olivier Saurel^{1,3}, Jerzy Czaplicki^{1,3}, J. Antoinette Killian⁴, Alain Milon^{1,3}*

1) Université de Toulouse-UPS; IPBS, 205 rte de Narbone, 31077 Toulouse, France;

2) Université de Toulouse-INSA-UPS, LPCNO, 135 av. de Rangueil 31077 Toulouse France3;

3) CNRS, UMR 5089 and UMR 5215, Toulouse, France;

4) Utrecht University, Chemical Biology and Organic Chemistry, Bijvoet Center for Biomolecular Research, Padualaan 8, 3584 CH Utrecht, The Netherlands.

A. Holt and L. Rougier contributed equally to this work

Keywords: solid state NMR, membrane, dynamics, anisotropic interactions, orientation, tilt angle

Running title: WALP peptide's dynamics by ssNMR

Abstract

A new solid-state NMR based strategy is established, for the precise and efficient analysis of orientation and dynamics of transmembrane peptides in fluid bilayers. For this purpose, several dynamically averaged anisotropic constraints, including ^{13}C and ^{15}N chemical shift anisotropies and ^{13}C - ^{15}N dipolar couplings were determined from two different triple isotope-labeled WALP23 peptides (^2H , ^{13}C , ^{15}N), and combined with previously published quadrupolar splittings of the same peptide. CSA tensor orientations were determined with quantum chemistry. The complete set of experimental constraints was analyzed using a generalized, 4-parameter, dynamic model of the peptide motion, including tilt and rotation angle and two associated order parameters. A tilt angle of 21° was determined for WALP23 in DMPC which is much larger than the tilt angle of 5.5° previously determined from ^2H NMR experiments. This approach provided a realistic value for the tilt angle of WALP23 peptide in the presence of hydrophobic mismatch, and can be generalized to any transmembrane helical peptide.

Introduction

In a number of recent publications the orientation of transmembrane peptides has been discussed, in particular in the context of hydrophobic mismatch (1, 2). The standard NMR method to probe the tilt and rotation angle of a peptide in a bilayer is based on the PISEMA (polarization inversion with spin exchange at magic angle (3)) experiment which measures ^{15}N chemical shift and ^{15}N -H dipolar coupling on each amide bond. More recently, as an alternative approach, the Geometric Analysis of Labeled Alanines (GALA) was developed, based on ^2H NMR quadrupolar splitting (4-6). With this method relatively small tilt angles (typically $5\text{-}10^\circ$, 5.5° for WALP23 in DMPC), were determined for WALP peptides, which are model peptides designed as mimics of α -helical transmembrane segments of membrane proteins. In a recent study ^{15}N PISEMA and ^2H GALA NMR approaches were compared on a similar peptide (GWALP23 in DLPC), yielding in both cases a fairly small tilt angle of around $13\text{-}10^\circ$, respectively (7). **Similar angle values were obtained by oriented CD (8) and in ATR-FTIR (9) spectroscopies.** These results are in apparent contradiction with recent molecular dynamics (MD) simulations which show that these transmembrane peptides are subject to large amplitude whole body motions and that they adopt large tilt angles, of e.g. $31^\circ \pm 12^\circ$ for WLP23 (10) or $33.5^\circ \pm 9^\circ$ (11) for WALP23 in DMPC. Although the authors of these MD simulations themselves point out some limitations, such as the length required to properly sample the peptide's behavior, the simulations clearly reveal that neglecting dynamical averaging in ^2H quadrupolar splitting interpretation leads to erroneous tilt angles. Therefore, an accurate analysis of the NMR data requires models which include dedicated peptide motions. It has been discussed already that dynamical averaging may be an important factor in the interpretation of PISEMA experiments (12, 13). Simulations of quadrupolar splitting of deuterated alanines in a peptide helix reveal that dynamical averaging has an even more pronounced effect on the quadrupolar splittings. This is illustrated in Figure 1.

Figure 1

Figure 1b shows that using the GALA approach (no wobbling, no oscillation) a larger tilt angle leads to a stronger variation of the quadrupolar splitting for various label positions. If oscillations about the long axis of the peptide are included into the simulations, these variations of the quadrupolar splitting are dampened. This behavior is illustrated in Figure 1c for a peptide with a tilt angle of 12° with $\Delta\rho$ varying from 1 to 150 degrees. In such a way averaging via oscillations is giving rise to an “apparent” tilt angle smaller than its actual value. Finally, in Figure 1d, wobbling-in-a-cone motions around the helix axis are also included into the simulations and it is shown that similar curves can be achieved for different sets of parameters.

From these simulations, it is obvious that quadrupolar splittings alone are not sufficient to distinguish various dynamical models as soon as wobbling and oscillations are taken into account, and that neglecting such peptide motions can lead to an underestimation of the tilt angle (such as 12° instead of 18°). Similar behavior was described recently in a study by Strandberg et al. (13). It is therefore essential to add different experimental anisotropic interactions (such as chemical shift anisotropy and dipolar coupling) when performing a

dynamical analysis. The recent work of Vostrikov et al. (7) is along this line by combining ^2H NMR and PISEMA experiments. However, the data were analyzed with a semi-static, 2-parameter model, with the associated artifacts illustrated above (the term “semi-static” is employed since a global, isotropic, order parameter, scaling down the NMR interaction is often included).

In the present study, we establish a new approach based on complementary anisotropic constraints to analyze the dynamics of membrane peptides. For this purpose, two triple isotope labeled WALP peptides have been synthesized. Additional anisotropic NMR parameters including two ^{15}N amide chemical shift anisotropies (CSAs), two ^{13}C carbonyl CSAs, two ^{15}N - ^{13}C dipolar couplings (DCs) between spins connected via the peptide bond were determined and combined with the six previously determined alanine methyl ^2H quadrupolar splittings (6). The previous deuterium NMR data already showed that the peptide is tilted (i.e. its most probable orientation is not the bilayer normal) and that fast axial diffusion is active along the bilayer normal but not along the α -helix axis (the bilayer normal is an axis of symmetry for the movement, the α -helix axis is not). Therefore a simple Maier-Saupe orienting potential(14) cannot be used to describe the peptide motion. The data analysis is thus based on a helix rigid body motion characterized by (see Figure 1a): (i) a fast axial diffusion of the peptide around the bilayer normal, (ii) an averaged position of the peptide in the bilayer defined by a tilt angle τ_0 (between the diffusion axis and the α -helix axis) and a rotation angle ρ_0 (around the α -helix axis), (iii) a wobbling amplitude $\Delta\tau$ around the averaged tilt angle τ_0 and (iv) an oscillation amplitude $\Delta\rho$ around the averaged rotation angle ρ_0 .

The anisotropic NMR interactions each explore a large range of orientations of the principal axis system (PAS) with respect to the helix axis, with the ^{15}N CSA being mostly sensitive to tilt and wobbling (as in the PISEMA approach) while the other anisotropic constraints are sensitive to a combination of the four parameters, each of them in a specific way. This appears to be essential for the identification of a unique motional model capable of fitting all the experimental data.

Materials & Methods

Materials: 1,2-dimyristoyl-*sn*-glycero-3-phosphocholine (DMPC) was obtained from Avanti Polar Lipids (Alabaster, AL) and used without further purification. Two different ^2H , ^{13}C , ^{15}N isotopically labeled WALP23 peptides (acetyl-GW2(LA)8LW2A-NH₂) were synthesized using Fmoc/tBu solid-phase synthesis, WALP23($^2\text{H}_3$ -Ala₁₃, $^{13}\text{C}_1$ -Ala₁₁, ^{15}N -Leu₁₂) referred to as WALP23#1 and WALP23($^2\text{H}_3$ -Ala₇, $^{13}\text{C}_1$ -Ala₁₃, ^{15}N -Leu₁₄) referred to as WALP23#2. Deuterium labeled L-alanine (3,3,3-*d*₃, 99%), $^{13}\text{C}_1$ labeled L-alanine (1- ^{13}C , 99%) and ^{15}N labeled L-leucine (^{15}N , 98%) were purchased from Cambridge Isotopes Laboratories Inc. (Andover, MA, USA). Fmoc (9-fluorenylmethyloxycarbonyl) was used to protect its amino functionality as described by (15) before being used in the peptide synthesis. The molecular mass of the synthesized peptides was verified by mass spectrometry and the

purity was analyzed by HPLC using a C4 reverse phase HPLC column. For analytical and, if necessary preparative, HPLC a solvent system with solvent A composed of 95% water, 5% acetonitrile and 0.1% TFA (trifluoroacetic acid), and solvent B composed of 80% acetonitrile, 20% iso-propanol and 0.1% TFA was used. The purity of the peptides used in this study was better than 95%.

NMR samples preparation: Static parameters of ^{15}N and ^{13}C anisotropic interactions were determined from lyophilysed WALP23 peptide; 6.5 μmol of powder of each peptide were packed into a 3.2 mm rotor. The ^2H static quadrupolar coupling constant of Ala methyl was measured on 60 mg of dry WALP23#2 peptide. WALP23 into LUVs of DMPC : Solutions of 20 mM DMPC in chloroform were prepared, and the lipid concentration was determined by the Rouser phosphorus assay. Solutions of WALP23 were prepared with a concentration of 500 μM in TFE (trifluoro ethanol) and the concentration of WALP23 was determined by absorption spectroscopy using an extinction coefficient of $22400\text{ M}^{-1}\text{cm}^{-1}$ at 280 nm. Unoriented samples i.e. liposomes were used instead of oriented bilayers to allow complete control of the hydration level. Typically 0.7 μmol of WALP23 peptides and 70 μmol DMPC were mixed in solution (1:100 peptide to lipid molar ratio). The organic solvents were evaporated under a nitrogen flow and further removed under vacuum overnight (ca. 10^{-2} mbar). Subsequently, the samples were hydrated with Milli-Q water and lyophilized to yield a fluffy powder, facilitating a thorough hydration at the low hydration levels needed. The unoriented samples were hydrated with deuterium-depleted water to 33% (water/(water+lipid+peptide), w/w) and incubated overnight at 37°C to equilibrate the hydration throughout the sample.

NMR experiments: Solid-state MAS (magic angle spinning) experiments were carried out on a Bruker Avance narrow-bore spectrometer operating at 700.13 MHz for ^1H . A Bruker 3.2 mm MAS triple-tuned solenoid coil was used for ^{13}C and ^{15}N experiments. Non-spinning ^2H and ^{15}N spectra were recorded on a Bruker Avance narrow-bore spectrometer operating at 500.13 MHz for ^1H with a 5 mm simple resonance and a 7 mm probe double resonance probe, respectively, both equipped with a solenoid coil oriented at 90° with respect to the magnetic field. The sample temperature was 313 K in every case. ^{13}C spectra were referenced to DSS and ^{15}N spectra to liquid ammonia, using the ^1H chemical shift of lipid's methyl resonances (0.85 ppm) as an internal reference for each nucleus.

^{13}C and ^{15}N static and averaged CSA parameters were determined from standard cross-polarization magic-angle spinning (CP-MAS) spectra. Isotropic chemical shifts were determined at a spinning frequency of 10 kHz. CSAs were recorded by spinning side band analyses. Typically, 4 kHz and 3 KHz were respectively used for the ^{13}C and ^{15}N static CSA determination while 0.75 kHz and 1kHz were used for the averaged CSA of WALP23 peptides into DMPC liposomes. ^{15}N CSA of WALP in lipid bilayers was also determined from the static NMR powder spectrum. ^{13}C - ^{15}N dipolar couplings were determined using a standard REDOR (16) experiment at a spinning frequency of 10 kHz, the $\Delta\text{S}/\text{S}_0$ REDOR curves were fitted in a standard manner (17) using Mathcad software (17-19). Deuterium NMR spectra were acquired using a standard quadrupolar echo pulse sequence (see supplementary material section for details on NMR experiments).

Determination of experimental static and dynamically averaged CSA: ^{13}C CSA parameters were obtained by the analysis of spinning sidebands intensity using dmfit freeware (<http://crmht-europe.cnrs-orleans.fr/dmfit/>). The static CSA and the asymmetry parameter were defined respectively as $\delta_{\text{aniso}} = \delta_{33} - \delta_{\text{iso}}$ and $\eta = (\delta_{22} - \delta_{11})/(\delta_{33} - \delta_{\text{iso}})$, with $|\delta_{33} - \delta_{\text{iso}}| \geq |\delta_{11} - \delta_{\text{iso}}| \geq |\delta_{22} - \delta_{\text{iso}}|$. The ^{13}C averaged CSA were determined by using a Hertzfeld-Berger analysis to extract the components of the ^{13}C dynamically averaged axially symmetric CSA defined as $\text{CSA}_{\text{exp}} = 3/2 (\delta_{90^\circ} - \delta_{\text{iso}})$ where δ_{90° is the chemical shift of peptide in membrane oriented at 90° with respect to the magnetic field and δ_{iso} is the isotropic chemical shift. ^{15}N averaged axially symmetric CSA_{exp} were determined from δ_{90° and δ_{iso} respectively measured on a powder static ^{15}N spectrum and on a CP-MAS spectrum at 10 kHz of spinning frequency (6).

Quantum chemistry calculation: The peptide's geometry and the ^{15}N and ^{13}C CSA static tensor components (more specifically principal axes orientation with respect to the helix geometry) are required for the calculation of dynamically averaged anisotropic interactions. Both the structure and the static theoretical NMR spectroscopic data were determined using a quantum chemical approach.

All quantum chemical calculations were performed using the Gaussian 03 suite of program (20). Molecular geometries of WALP23 were optimized starting from a perfect canonical α helix structure ($\Phi = -58^\circ$ and $\Psi = -47^\circ$) using the ONIOM hybrid approach (21, 22) that divides the system in an "active" and an "inactive" part. The active part (7 residues centered on Ala11-Leu12 or Ala13-Leu14 peptide bond) was calculated using the hybrid Density Functional Theory B3LYP method (23, 24) associated with a Pople type double ξ basis set augmented by polarization functions on all atoms (namely 6-31G(d,p)) (25). The inactive part of the system (the rest of the peptide) was calculated using a semi-empirical (AM1) approach (26-28). NMR chemical shielding tensors were computed at the B3LYP/6-31G(d,p) level of theory on the whole peptide using the Gauge Including Atomic Orbital method (GIAO) for the numerous advantages it offers (29-33).

In order to allow the calculation of motionally averaged CSA parameters, the molecular frame (M) was chosen as follows: the z axis is the main inertia axis of the α -helix; the x -axis is perpendicular to the z -axis and contains the Leu₁₂ α -carbon; the y -axis completes the direct orthonormal frame. Thus α_{PM}^{CSA} , β_{PM}^{CSA} and γ_{PM}^{CSA} angles given in Table 2 (results and discussion section) are the Euler angles associated with the rotation matrix between the CSA tensor principal axis system PAS and the molecular frame M using the zyz convention. ^{15}N - $^{13}\text{C}_1$ dipolar coupling and methyl Ala ^2H quadrupolar coupling tensor orientations are defined by the spherical coordinates (Theta and Phi) of the ^{13}C - ^{15}N and C_α - C_β bond in the molecular frame. The associated numerical values were extracted from the quantum chemical optimized geometries.

Computation of the dynamically averaged anisotropic interactions and experimental fittings: Using the static anisotropic tensor information obtained as described above, dynamically averaged interactions were computed using a four-parameter model of motion involving tilt (τ_0), wobbling in a cone of angle $\Delta\tau$, rotation (ρ_0) and oscillation of amplitude

$\Delta\rho$ (see figure 1a). Internal dynamics of the peptide's helical structure, although certainly present, were assumed to be negligible, based on the observation by molecular dynamics that the helical structure is well preserved during the simulations (11).

Both quadrupolar and dipolar splittings were computed from the expression:

$$g(\beta_{PN}^{QC/DC}) = K_{QC/DC} \cdot \frac{3\cos^2 \beta_{PN}^{QC/DC} - 1}{2}$$

where the constant $K_{QC/DC}$ depends on the type of interaction, quadrupolar (QC) or dipolar coupling (DC), respectively. $\beta_{PN}^{QC/DC}$ defines the orientation of the bilayer normal \vec{N} relative to the principal axis frame of dipolar or quadrupolar interaction tensor (C-D quadrupolar tensor being quasi axially symmetric). This equation is given for bilayers oriented with the bilayer normal parallel to the magnetic field.

The Chemical Shift Anisotropy (CSA) effects depend on the spherical coordinates β_{PN}^{CSA} and α_{PN}^{CSA} of the bilayer normal \vec{N} in the principal axis frame (PAF) of the CSA tensor (where η is the asymmetry parameter):

$$h(\beta_{PN}^{CSA}, \alpha_{PN}^{CSA}) = -K_{CSA} \cdot \left[\left(\frac{3\cos^2 \beta_{PN}^{CSA} - 1}{2} \right) + \frac{1}{2} \eta (\sin^2 \beta_{PN}^{CSA} \cos 2\alpha_{PN}^{CSA}) \right]$$

Following the Wigner rotation matrix formalism (34), equations $g(\beta_{PN}^{QC/DC})$ and $h(\beta_{PN}^{CSA}, \alpha_{PN}^{CSA})$ were expressed as function of the PAS orientation relative to the molecular frame (noted M) and M frame orientation relative to the diffusion frame (noted N).

Peptide motion in the sub-microsecond time scale leads to time-modulated β_{PN}^i and α_{PN}^i angles, and was included by integrating $g(\beta_{PN}^{QC/DC})$ and $h(\beta_{PN}^{CSA}, \alpha_{PN}^{CSA})$ over the angles describing the movements i.e. variation of τ between $\tau_0 - \Delta\tau$ and $\tau_0 + \Delta\tau$ and of ρ between $\rho_0 - \Delta\rho$ and $\rho_0 + \Delta\rho$, as described in supplementary material section.

The dynamically averaged theoretical anisotropic interactions (QCs, DCs and CSAs) were then calculated and compared to the experimental data. The sum of their squared differences was minimized to obtain the best fit. In order to avoid the traps of local minima typical for gradient-based approaches, we have used GOSA (35), a multivariate global optimization program based on simulated annealing (<http://www.bio-log.biz>). To estimate errors of the best-fit parameters, a Monte Carlo approach was employed (36). A set of 100 combinations of experimental values was randomly generated within the limits of experimental errors, and the fit was performed for each of them. This gave a representation of multiple minima in the four-parameter space (such as lines F1 and F2 in Table 3), and the range of possible values for each fitted parameter. Multidimensional integration was performed with the CUBA library (37).

Results & Discussion

Secondary structure and aggregation state of WALP23: For interpretation of the solid state NMR data in terms of a structural and dynamic model of WALP23, it first is important to

know whether under the experimental conditions used, the peptide can be considered as a monomeric and stable helix, diffusing freely in the fluid bilayer.

Different studies have shown the backbone structure of the WALP peptides to be remarkably robust, even withstanding considerable mismatch. This is most clear from FTIR measurements, which showed an intense narrow band at the amide I position of a range of different length WALP peptides, which did not shift or broaden upon either increasing or decreasing bilayer thickness(9). Also CD measurements(9, 38) showed an α -helical structure under a range of conditions, and fits of ^2H NMR data on Ala-d4 labeled peptides suggested significant distortion only at conditions of extreme positive mismatch(39). Also a variety of MD simulations suggested a rather perfect and robust α -helix(11, 40). With respect to the aggregational behavior, it should be mentioned that different lines of experimental evidence suggest that WALP23 by itself has no tendency to self-associate in a lipid bilayer. For example: the lipid flip-flop promoting effect of the peptides was found to be perfectly linear over a wide range of peptide concentrations(41), self-quenching of pyrene labeled peptides was found to occur only at peptide concentrations significantly higher than those in the present study(42), and the same holds for sucrose density gradient centrifugation experiments which showed homogeneous peptide/lipid mixtures up to very high peptide/lipid ratio's(38). So far only in the gel phase of DPPC and other saturated lipids aggregates have been observed by AFM. However, these were linear aggregates, supporting in fact the notion that the peptides have a strong preference for interaction with lipids(43). Nevertheless to avoid any risk of peptide aggregation, we performed our analysis on samples with a relatively low peptide/lipid ratio of 1/100.

Static ^{13}C and ^{15}N CSA tensor parameters computed by quantum chemistry: Static ^{13}C and ^{15}N CSAs and asymmetry parameters were found to be close to the experimental values obtained on dry peptide. Consequently, we can be confident on their correctness and in particular on the quality of the eigenvectors (tensor orientation relative to the molecular frame, see Table 1). In order to check the accuracy of our theoretical chemical shielding eigenvectors, we can define the tensor orientation relative to the peptide plane (Figure 2 and Table 1).

Figure 2

Table 1

For the ^{15}N tensor, α_{N} is the angle between e_{11} and the $\text{N}^i\text{-C}^{i-1}$ peptide bond, β_{N} the angle between e_{22} and the normal to the peptide plane and γ_{N} , the angle between e_{33} and the N-H bond where e_{ii} is the eigenvector associated with the σ_{ii} eigenvalue (see Figure 3 for e_{ii} representation). For the $^{13}\text{C}_1$ tensor, α_{C} is the angle between e_{11} and the $\text{N}^i\text{-C}^{i-1}$ peptide bond, β_{C} the angle between e_{22} and the CO bond and γ_{C} , the angle between e_{33} and the normal to the peptide plane. The angles obtained on both peptides (see Table 1) are in agreement with the standard values used to describe ^{15}N and ^{13}C chemical shift tensor eigenvectors (44-46). Particularly, for ^{15}N , the angle between e_{33} and the N-H bond is equal to 19° and the e_{11} is

tilted by about 21° from the peptide plane. For $^{13}\text{C}_1$, the α_{C} angle is close to 32° , e_{22} is almost collinear to the carbonyl CO bond and e_{33} is perpendicular to the peptide plane.

MAS NMR experiments on peptides inserted into membranes : To ensure compatibility of the existing ^2H NMR data with the new NMR data, a deuterium labeled Alanine was included in each peptide, which allowed checking the sample conditions by deuterium NMR. For both triple-labeled peptides, the quadrupolar splitting found were identical to the previously published values (6) (data not shown). In addition, each sample permitted the determination of ^{15}N amide chemical shift and averaged CSA for one Leucine, ^{13}C carbonyl chemical shift and averaged CSA for one Alanine (Figure 3), and one ^{15}N - ^{13}C dipolar coupling linked to the dynamics and orientation of the N-C₁ peptide bond (data not shown).

Figure 3

Isotropic chemical shifts were determined at a spinning frequency of 10 kHz on both peptides inserted into bilayers. The carbonyl ^{13}C linewidths were equal to 0.3 ppm which is a good indication of structural homogeneity. The isotropic ^{13}C chemical shift, 178.9 ppm in both cases, was typical for a peptide in a helical conformation confirming that the peptide's dynamics preserves a helical conformation at positions 11 and 13.

In order to determine dynamically averaged CSAs, two strategies were applied depending on spectral overlap and sensitivity of each nucleus. For ^{13}C , dynamically averaged CSAs were obtained from slow spinning sideband MAS spectra analysis, which allows resolving resonances arising from the peptides and those arising from natural abundance lipid carbonyls (see Figure 3a). For ^{15}N dynamically averaged CSAs, the most efficient method, due to the low signal intensity, appeared to be the comparison between the isotropic chemical shift measured under MAS conditions and the powder spectrum measured under static conditions. The most intense shoulder of the powder spectrum provides the value of δ_{90° (Figure 3b) as was already proposed for axially diffusing peptides in (47). The magic-angle hole can be seen in ^{15}N static spectra and results from the colinearity of the chemical shift tensor and the dipolar coupling tensor in uniaxially mobile molecules (48).

The CSA values for both ^{15}N and ^{13}C confirm the dynamical behavior of the peptide, since they are significantly lower in liposomes than in peptide powder (compare for example Figures 3a with 3c and 3b with 3d, and values in Table 2). Moreover, the asymmetry parameters extracted from spinning sideband analysis of the ^{13}C spectra were found to be null for both peptides in liposomes, in agreement with dynamics involving fast axial diffusion along the bilayer normal, as was already demonstrated in previous ^2H NMR experiments (5, 6). The resulting part of the anisotropic interaction is directly related to the peptide's motion in terms of tilt (τ_0), rotation (ρ_0), wobbling ($\Delta\tau$) and oscillation ($\Delta\rho$). All the computed static and experimentally determined static and dynamically averaged CSAs are summarized in Table 2, together with quadrupolar and dipolar splittings.

Table 2

Data analysis and extraction of dynamical parameters: Six new anisotropic constraints have been determined and were combined with the previously published 6 quadrupolar splittings determined on peptides including deuterated alanines. As described in materials and methods section, we then explored the entire space of possible solutions in terms of a four-parameter dynamical model involving tilt τ_0 , rotation ρ_0 , wobbling $\Delta\tau$ and oscillations $\Delta\rho$. In the fitting procedure, the principal axes orientation were taken from computed values, while the principal values were the experimental ones, measured on the dry peptide powder by standard spinning sideband analysis (see Table 2). The complementary orientations of the anisotropic tensors allowed identifying a well defined region of agreement between simulations and experiment, as illustrated in Figure 4 and in Table 3, line A.

Figure 4

Table 3

Several important conclusions can be drawn from this analysis:

a) The complete set of anisotropic constraints is sufficient to extract the complete orientation and dynamics of the WALP peptide in DMPC (Table 3, line A). The tilt and rotation angles are determined with a good accuracy (20.8 ± 1.4 and 146 ± 7 degrees respectively), which agrees well with the tilt angle of 23° obtained recently using a fluorescence approach (49) and confirms the trends indicated in molecular dynamics simulations (11). Although the qualitative agreement with fluorescence and MD simulation is interesting, it should be realized that these two approaches each have their own limitations, and we believe the present NMR approach to be more accurate. In particular, the MD work is on a completely different timescale and the motions seen by MD may or may not accurately reflect the population examined on the timescale of the NMR experiment. Our NMR analysis furthermore shows that both the tilt and rotation angles are very stable among the various subsets of constraints (lines A to E). The wobbling and oscillation amplitudes are also determined with a reasonable accuracy, although slightly less precisely than tilt and rotation. The oscillation amplitude $\Delta\rho$ is very large ($\pm 84^\circ$), confirming that data analysis based on a semi-static, 2-parameter model is inappropriate. The order of magnitude of $\Delta\rho$ is in complete agreement with the molecular dynamics simulation (11, 50). Compared with the GALA analysis it should be stressed that the rotation angle ρ_0 initially determined is not modified. The angle of 155° , as determined in Ozdirekcan et al. corresponds to 145° in the molecular frame used in the present paper, and hence corresponds well with the value of 146° obtained here. These results show that dynamical averaging mostly affects the tilt angle determination.

b) ^{15}N - ^{13}C dipolar couplings obtained for this highly dynamic peptide are weak (~ 300 Hz). The accuracy is relatively low due to the low signal to noise ratio. Removal of these constraints does not significantly change the outcome of the fit (line B), suggesting to proceed with the analysis without parameters from the fairly time-consuming REDOR experiments.

c) Adding ^{15}N -H dipolar couplings such as those which can be measured from the (also time consuming) PISEMA experiment, does not add much to the data analysis (line C). This can be understood from the fact that the main tensor orientation of ^{15}N -H dipolar coupling and ^{15}N CSA interactions are similar, i.e. almost parallel to the helix axis. Both are very

sensitive to the helix tilt (τ_0 and $\Delta\tau$), and less sensitive to helix rotation (ρ and $\Delta\rho$). Therefore using only these two interactions is not sufficient for accurate data analysis (see **H** where τ_0 , $\Delta\tau$, ρ_0 are different and where $\Delta\rho$ is not determined), but using one of them is necessary (and sufficient) to separate the two pairs of variables. Accordingly, using only the six CD_3 quadrupolar splittings and two ^{15}N CSA values gives a good solution to the problem (**E**), while six quadrupolar splittings alone are not sufficient (**F1** and **F2**, note that the best fitting in that case is obtained for F1, i.e. for a very small tilt angle). It should be stressed that the PISEMA experiment offers the advantage of a 2D experiment in terms of increased resolution, and thus allows obtaining exploitable anisotropic interactions on uniformly ^{15}N -labeled peptides.

d) About exploring various motional models: largely similar conclusions were derived when a Gaussian distribution was used instead of a uniform distribution. In the case of the Gaussian distributions a global minimum was found for $\tau_0 = 16.2^\circ \pm 1.6^\circ$, $\Delta\tau = 12.0^\circ \pm 1.6^\circ$, $\rho_0 = 146.6^\circ \pm 15.4^\circ$, $\Delta\rho = 98.2^\circ \pm 5.5^\circ$. Hence a slightly smaller tilt angle was found, and the other parameters were well within the experimental error. Although MD simulations show that the helical structure is very stable (11, 40, 51), internal dynamics of the peptide is also expected to influence the data analysis to some extent. This point is currently under examination by assessing such “internal order parameters” from MD simulations and by incorporating them into the data fitting process.

e) In search for an optimal strategy to do a dynamical analysis of a transmembrane peptide (with fast axial diffusion around the bilayer normal), we propose to use 6 anisotropic interactions which allow sampling optimally different tensor orientations by selecting specific labeling positions along the peptide helix (line **D** of Table 3). Thus, accurate dynamic analysis is already possible by synthesizing only two different triply labeled peptides, each of which includes a ^2H (CD_3 on Ala₁₁ or 13), a $^{13}\text{C}_1$ (Ala₁₁ or 13) and a ^{15}N (Leu₁₂ or 14) label, which would require about 3-4 days measurement time on a 500 to 700 MHz solid state NMR spectrometer.

f) About description of the motion in terms of order parameters: following the notation of Goormaghtigh et al. (52) one can convert the values of τ_0 and of $\Delta\tau$ into values of order parameters. The distribution of helix axis can be described by the product of two order parameters: $S_{\text{helix}} = S_{\text{helix angle}} \cdot S_{\text{helix order}}$

$S_{\text{helix angle}} = \langle 3\cos^2(\tau_0) - 1 \rangle / 2$ is related to the average tilt angle τ_0

$S_{\text{helix order}} = \langle 3\cos^2(\tau_1) - 1 \rangle / 2$ related to the wobbling ($\langle \rangle = \text{average over } \tau_1 \in [0, \Delta\tau]$)

(see supporting information for the angle definitions).

For the uniform distribution, the values $\tau_0 = 20.8^\circ$ and $\Delta\tau = 12.2^\circ$ translate into

$S_{\text{helix angle}} = 0.81$, $S_{\text{helix order}} = 0.97$, and $S_{\text{helix}} = 0.78$

This value of $S_{\text{helix order}}$ is significantly higher than the molecular order parameter S_{zz} of a DPPC (53) or DMPC (54) lipid in the fluid phase which is around 0.6. This is not surprising considering that the peptide is anchored on both sides of the bilayer while the lipid molecules extend over only half of the bilayer.

Several methods have been used to study structural properties of membrane proteins and to determine tilt angle of transmembrane peptides, including solid-state NMR, EPR, CD, ATR-

FTIR and fluorescence spectroscopies (for a recent review see A. Holt and A. Killian, Eur. Biophys. J., in press, 2010). All these techniques, like ^2H GALA NMR, are powerful and simple to interpret in terms of an averaged orientation of the helices (τ_0 , ρ_0). However, the existence of distributions of orientation (characterized by a wobbling $\Delta\tau$ and oscillation $\Delta\rho$ parameters) and averaging effects make things more difficult. For instance, it is clearly stated in the very comprehensive review of Goormaghtigh et al. (52) that in the usual data treatment of ATR IR spectroscopy “ $S_{\text{helix order}}$ cannot be evaluated independently from $S_{\text{helix angle}}$ ”, so that usually $S_{\text{helix order}}$ is set to 1 (i.e. $\Delta\tau=0$). Moreover, in the case of WALP23, one has to deal with the existence of a non axially symmetric distribution of the rotation angle ρ and the associated “amplitude of oscillations” ($\Delta\rho$), and this had never been included in the data analysis for a tilted peptide, to the best of our knowledge.

Conclusions

In the present work we analyzed data set of different NMR anisotropic interactions (quadrupolar couplings, dipolar couplings and chemical shift anisotropies) with an extended, dynamical four-parameter (τ_0 , $\Delta\tau$, ρ_0 , $\Delta\rho$) peptide model. An averaged tilt angle of 21° for WALP23 peptides inserted into DMPC has been determined. This is much larger than the tilt angle of 5.2° obtained by ^2H GALA NMR analysis based on a quasi static model and follows the trends towards larger tilt angles as indicated from MD simulations. It also provides an accurate determination of rotation angle, wobbling and oscillation amplitudes. It does not give however any indication on the various time scales of these motions. These could be obtained in principle by analyzing solid state deuterium NMR inversion-recovery and Jeener-broekaert relaxation data in a similar way to the one proposed by Prosser et al for lipids (55) or for the peptide gramicidin (14). ^1H , ^{13}C and ^{15}N relaxation studies in the rotation frame under magic angle spinning and with static oriented sample could also be used to characterize the motional model (56). It should be stressed however that for this particular case, the motional model should include at least three time scales, characterizing diffusion along the bilayer normal, wobbling and oscillations (not counting slow ensemble motions of the bilayer).

In the strategy, the combination of at least three different anisotropic tensors, possessing complementary orientations, proved to be essential to solve the inherent undetermination brought by the explicit introduction of dynamical averaging and to analyze the orientation and dynamics of transmembrane peptides in a precise and efficient way. This approach should be very generally applicable to any transmembrane peptide and will allow assessing the influence of hydrophobic mismatch, not only on tilt angles but also on the amplitudes of wobbling and oscillations.

Acknowledgment: The authors wish to acknowledge financial supports from the European Marie Curie program for A.H. (BIOMEM, Contract MEST-CT 2004-007931), and from “Conseil Régional Midi-Pyrénées” and PRES “Université de Toulouse” to L.R.. We thank the

“CALcul en Midi-Pyrénées” (CALMIP) computing center for generous allocations of computer time. We thank Rutger Staffhorst, Jacques Doux and Lucie Khemtémourian for peptide synthesis. The NMR spectra were recorded on spectrometers financed with the help of European Structural funds, Région Midi-Pyrénées and CNRS.

References

1. Hong, M. 2007. Structure, topology, and dynamics of membrane peptides and proteins from solid-state NMR Spectroscopy. *J. Phys. Chem. B* 111:10340-10351.
2. Nyholm, T. K. M., S. Ozdirekcan, and J. A. Killian. 2007. How protein transmembrane segments sense the lipid environment. *Biochemistry* 46:1457-1465.
3. Cross, T. A., and S. J. Opella. 1994. Solid-State NMR Structural Studies of Peptides and Proteins in Membranes. *Curr. Opin. Struct. Biol.* 4:574-581.
4. Jones, D. H., K. R. Barber, E. W. VanDerLoo, and C. W. M. Grant. 1998. Epidermal growth factor receptor transmembrane domain: H-2 NMR implications for orientation and motion in a bilayer environment. *Biochemistry* 37:16780-16787.
5. van der Wel, P. C. A., E. Strandberg, J. A. Killian, and R. E. Koeppe. 2002. Geometry and intrinsic tilt of a tryptophan-anchored transmembrane alpha-helix determined by H-2 NMR. *Biophys. J.* 83:1479-1488.
6. Strandberg, E., S. Ozdirekcan, D. T. S. Rijkers, P. C. A. van der Wel, R. E. Koeppe, R. M. J. Liskamp, and J. A. Killian. 2004. Tilt angles of transmembrane model peptides in oriented and non-oriented lipid bilayers as determined by H-2 solid-state NMR. *Biophys. J.* 86:3709-3721.
7. Vostrikov, V. V., C. V. Grant, A. E. Daily, S. J. Opella, and R. E. Koeppe. 2008. Comparison of "Polarization Inversion with Spin Exchange at Magic Angle" and "Geometric Analysis of Labeled Alanines" methods for transmembrane helix alignment. *J. Am. Chem. Soc.* 130:12584-12585.
8. de Planque, M. R., J. A. Kruijtzter, R. M. Liskamp, D. Marsh, D. V. Greathouse, R. E. Koeppe, 2nd, B. de Kruijff, and J. A. Killian. 1999. Different membrane anchoring positions of tryptophan and lysine in synthetic transmembrane alpha-helical peptides. *J. Biol. Chem.* 274.
9. de Planque, M. R. R., E. Goormaghtigh, D. V. Greathouse, R. E. Koeppe, J. A. W. Kruijtzter, R. M. J. Liskamp, B. de Kruijff, and J. A. Killian. 2001. Sensitivity of single membrane-spanning alpha-helical peptides to hydrophobic mismatch with a lipid bilayer: Effects on backbone structure, orientation, and extent of membrane incorporation. *Biochemistry* 40:5000-5010.
10. Esteban-Martin, S., and J. Salgado. 2007. The dynamic orientation of membrane-bound peptides: Bridging simulations and experiments. *Biophys. J.* 93:4278-4288.
11. Ozdirekcan, S., C. Etchebest, J. A. Killian, and P. F. J. Fuchs. 2007. On the orientation of a designed transmembrane peptide: Toward the right tilt angle? *J. Am. Chem. Soc.* 129:15174-15181.
12. Straus, S. K., W. R. Scott, and A. Watts. 2003. Assessing the effects of time and spatial averaging in 15N chemical shift/15N-1H dipolar correlation solid state NMR experiments. *J. Biomol. NMR* 26:283-295.
13. Strandberg, E., S. Esteban-Martin, J. Salgado, and A. S. Ulrich. 2009. Orientation and Dynamics of Peptides in Membranes Calculated from H-2-NMR Data. *Biophys. J.* 96:3223-3232.
14. Prosser, R. S., and J. H. Davis. 1994. Dynamics of an Integral Membrane Peptide - a Deuterium Nmr Relaxation Study of Gramicidin. *Biophys. J.* 66:1429-1440.
15. Tenkortenaar, P. B. W., B. G. Vandijk, J. M. Peeters, B. J. Raaben, P. J. H. M. Adams, and G. I. Tesser. 1986. Rapid and Efficient Method for the Preparation of Fmoc-Amino Acids Starting from 9-Fluorenylmethanol. *Int. J. Pept. Prot. Res.* 27:398-400.
16. Gullion, T., and J. Schaefer. 1989. Rotational-Echo Double-Resonance NMR. *J. Magn. Reson.* 81:196-200.

17. Gullion, T., and J. Schaefer. 1989. Rotational-Echo Double-Resonance NMR. *Adv. Magn. Reson.* 13:57.
18. Mathcad. 1986-2000. *MathSoft, Inc.*
19. Gullion, T., D. B. Baker, and M. S. Conradi. 1990. New, Compensated Carr-Purcell Sequences. *J. Magn. Reson.* 89:479-484.
20. Gaussian 03 Revision E.01.1 Frisch, M. J., et al. *Gaussian, Inc, Wallingford CT, 2004.*
21. Maseras, F., and K. Morokuma. 1995. Imomm - a New Integrated Ab-Initio Plus Molecular Mechanics Geometry Optimization Scheme of Equilibrium Structures and Transition-States. *J. Comput. Chem.* 16:1170-1179.
22. Vreven, T., and K. Morokuma. 2000. On the application of the IMOMO (integrated molecular orbital plus molecular orbital) method. *J. Comput. Chem.* 21:1419-1432.
23. Becke, A. D. 1993. Density-Functional Thermochemistry .3. The Role of Exact Exchange. *J. Chem. Phys.* 98:5648-5652.
24. Lee, C., W. Yang, and R. G. Parr. 1988. Development of the Colle-Salvetti correlation-energy formula into a functional of the electron density. *Phys. Rev. B* 37:785.
25. Foresman, A. E. 1998. In Exploring chemistry with electronic structure methods. Gaussian Inc., Pittsburgh.
26. Dewar, M. J. S., M. L. McKee, and S. Rzepa. 1978. Mndo Parameters for 3rd Period Elements. *J. Am. Chem. Soc.* 100:3607.
27. Dewar, M. J. S., and W. Thiel. 1977. Mindo-3 Study of Addition of Singlet Oxygen Delta-G-1o-2 to 1,3-Butadiene. *J. Am. Chem. Soc.* 99:2338.
28. Anders, E., R. Koch, and P. Freunsch. 1993. Optimization and Application of Lithium Parameters for Pm3. *J. Comput. Chem.* 14:1301-1312.
29. Wolinski, K., and A. J. Sadlej. 1980. Self-Consistent Perturbation-Theory - Open-Shell States in Perturbation-Dependent Non-Orthogonal Basis-Sets. *Mol Phys* 41:1419-1430.
30. Wolinski, K., J. F. Hinton, and P. Pulay. 1990. Efficient Implementation of the Gauge-Independent Atomic Orbital Method for Nmr Chemical-Shift Calculations. *J. Am. Chem. Soc.* 112:8251-8260.
31. Ditchfield, R. 1974. Self-consistent perturbation theory of diamagnetism I. A gauge-invariant LCAO method for N.M.R. chemical shifts. *Mol. Phys.* 27:789.
32. McWeeny, R. 1962. Perturbation Theory for the Fock-Dirac Density Matrix. *Phys. Rev.* 126:1028.
33. London, F. J. 1937. Théorie quantique des courants interatomiques dans les combinaisons aromatiques. *J. Phys. Radium* 8:397.
34. Schmidt-Rohr, K., and H. W. Spiess. 1994. In Multidimensional solid-state NMR and polymers. A. Press, editor. Harcourt Brace & Company, London. 444-452.
35. Czaplicki, J., G. Cornélissen, and F. F. Halberg. 2006. GOSA, a simulated annealing-based program for global optimization of nonlinear problems, also reveals transyears. *J. Appl. Biomed.* 4:87-94.
36. Bevington, P., and D. K. Robinson. 2002. Data Reduction and Error Analysis for the Physical Sciences. McGraw-Hill.
37. Hahn, T. 2005. CUBA - a library for multidimensional numerical integration. *Comput. Phys. Commun.* 168:78-95.
38. Killian, J. A., I. Salemink, M. R. R. dePlanque, G. Lindblom, R. E. Koeppe, and D. V. Greathouse. 1996. Induction of nonbilayer structures in diacylphosphatidylcholine model membranes by transmembrane alpha-helical peptides: Importance of hydrophobic mismatch and proposed role of tryptophans. *Biochemistry* 35:1037-1045.

39. Daily, A. E., D. V. Greathouse, P. C. A. van der Wel, and R. E. Koeppe. 2008. Helical distortion in tryptophan- and lysine-anchored membrane-spanning alpha-helices as a function of hydrophobic mismatch: A solid-state deuterium NMR investigation using the geometric analysis of labeled alanines method. *Biophys. J.* 94:480-491.
40. Ulmschneider, J. P., J. P. F. Doux, J. A. Killian, J. C. Smith, and M. B. Ulmschneider. 2009. Peptide Partitioning and Folding into Lipid Bilayers. *J. Chem. Theory Comput.* 5:2202–2205.
41. Kol, M. A., A. N. C. van Laak, D. T. S. Rijkers, J. A. Killian, A. I. P. M. de Kroon, and B. de Kruijff. 2003. Phospholipid flop induced by transmembrane peptides in model membranes is modulated by lipid composition. *Biochemistry* 42:231-237.
42. Sparr, E., W. L. Ash, P. V. Nazarov, D. T. S. Rijkers, M. A. Hemminga, D. P. Tieleman, and J. A. Killian. 2005. Self-association of transmembrane alpha-helices in model membranes - Importance of helix orientation and role of hydrophobic mismatch. *J. Biol. Chem.* 280:39324-39331.
43. Sparr, E., D. N. Ganchev, M. M. E. Snel, A. N. J. A. Ridder, L. M. J. Kroon-Batenburg, V. Chupin, D. T. S. Rijkers, J. A. Killian, and B. de Kruijff. 2005. Molecular organization in striated domains induced by transmembrane alpha-helical peptides in dipalmitoyl phosphatidylcholine bilayers. *Biochemistry* 44:2-10.
44. Hartzell, C. J., M. Whitfield, T. G. Oas, and G. P. Drobny. 1987. Determination of the N-15 and C-13 Chemical-Shift Tensors of L- C-13 Alanyl-L- N-15 Alanine from the Dipole-Coupled Powder Patterns. *J. Am. Chem. Soc.* 109:5966-5969.
45. Marassi, F. M. 2002. NMR of peptides and proteins in oriented membranes. *Concepts Magn. Resonance* 14:212-224.
46. Wu, C. H., A. Ramamoorthy, L. M. Gierasch, and S. J. Opella. 1995. Simultaneous Characterization of the Amide H-1 Chemical Shift, H-1-N-15 Dipolar, and N-15 Chemical-Shift Interaction Tensors in a Peptide-Bond by 3-Dimensional Solid-State Nmr-Spectroscopy. *J. Am. Chem. Soc.* 117:6148-6149.
47. Cady, S. D., C. Goodman, C. D. Tatko, W. F. DeGrado, and M. Hong. 2007. Determining the orientation of uniaxially rotating membrane proteins using unoriented samples: A H-2, C-13, and N-15 solid-state NMR investigation of the dynamics and orientation of a transmembrane helical bundle. *J. Am. Chem. Soc.* 129:5719-5729.
48. Yamaguchi, S., D. Huster, A. Waring, R. I. Lehrer, W. Kearney, B. F. Tack, and M. Hong. 2001. Orientation and dynamics of an antimicrobial peptide in the lipid bilayer by solid-state NMR spectroscopy. *Biophys. J.* 81:2203-2214.
49. Holt, A., R. B. M. Koehorst, T. Meijneke, M. H. Gelb, D. T. Rijkers, M. A. Hemminga, and J. A. Killian. 2009. Tilt and rotation angles of a transmembrane model peptide as studied by fluorescence spectroscopy. *Biophys. J.* 97:2258-2266.
50. Ozdirekcan, S., D. T. S. Rijkers, R. M. J. Liskamp, and J. A. Killian. 2005. Influence of flanking residues on tilt and rotation angles of transmembrane peptides in lipid bilayers. A solid-state H-2 NMR study. *Biochemistry* 44:1004-1012.
51. Shi, L., A. Cembran, J. L. Gao, and G. Veglia. 2009. Tilt and Azimuthal Angles of a Transmembrane Peptide: A Comparison between Molecular Dynamics Calculations and Solid-State NMR Data of Sarcolipin in Lipid Membranes. *Biophys. J.* 96:3648-3662.
52. Goormaghtigh, E., V. Raussens, and J. M. Ruysschaert. 1999. Attenuated total reflection infrared spectroscopy of proteins and lipids in biological membranes. *BBA Rev. Biomembranes* 1422:105-185.
53. Prosser, R. S., J. H. Davis, C. Mayer, K. Weisz, and G. Kothe. 1992. Deuterium NMR relaxation studies of peptide-lipid interactions. *Biochemistry* 31:9355-9363.

54. Mayer, C., G. Grobner, K. Muller, K. Weisz, and G. Kothe. 1990. Orientation-dependent deuteron spin-lattice relaxation-times in bilayer membranes - Characterization of the overall lipid motion. *Chem. Phys. Lett.* 165:155-161.
55. Prosser, R. S., J. H. Davis, C. Mayer, K. Weisz, and G. Kothe. 1992. Deuterium Nmr Relaxation Studies of Peptide-Lipid Interactions. *Biochemistry* 31:9355-9363.
56. Fares, C., J. Qian, and J. H. Davis. 2005. Magic angle spinning and static oriented sample NMR studies of the relaxation in the rotating frame of membrane peptides. *J. Chem. Phys.* 122:194908.

^{13}C	α_{C}	β_{C}	γ_{C}
Ala ₁₁	32.2	2.1	2.1
Ala ₁₃	31.8	2.4	2.0
^{15}N	α_{N}	β_{N}	γ_{N}
Leu ₁₂	20.9	17.9	19.2
Leu ₁₄	20.7	17.7	19.5

Table 1: Chemical shift tensor orientation relative to the peptide plan computed for WALP23 peptide. See text for details on definition of angles

Chemical shift tensors						
	δ_{aniso}^*	η^*	$\alpha_{PM}^{\text{CSA}\dagger}$	$\beta_{PM}^{\text{CSA}\dagger}$	$\gamma_{PM}^{\text{CSA}\dagger}$	$CSA\text{ exp}^{\ddagger}$
	(ppm)		($^{\circ}$)	($^{\circ}$)	($^{\circ}$)	(ppm)
[^{13}C]Ala ₁₁	-84.2	0.59	-82.0	97.7	323.3	-16.4 ± 1.6
[^{13}C]Ala ₁₃	-85.1	0.62	-77.9	102.7	135.8	-20.1 ± 2.0
[^{15}N]Leu ₁₂	104.6	0.20	-163.3	15.1	20.5	-105.6 ± 5.0
[^{15}N]Leu ₁₄	104.5	0.19	-138.0	15.6	168.0	-114.6 ± 5.0
Dipolar interactions						
	K^*		Theta \dagger	Phi \dagger		$DC\text{ exp}^{\ddagger}$
	(Hz)		($^{\circ}$)	($^{\circ}$)		(Hz)
[^{13}C]Ala ₁₁ -[^{15}N]Leu ₁₂	1010		68.9	312.4		313 ± 100
[^{13}C]Ala ₁₃ -[^{15}N]Leu ₁₄	1010		69.3	114.6		286 ± 100
Quadrupolar interactions						
	K^*		Theta \dagger	Phi \dagger		$\Delta\nu_Q^{\ddagger}$
	(Hz)		($^{\circ}$)	($^{\circ}$)		(Hz)
CD ₃ -Ala ₇	37700		58.7	85.5		500 ± 500
CD ₃ -Ala ₉	37700		58.1	247.8		5725 ± 500
CD ₃ -Ala ₁₁	37700		58.7	50.3		1000 ± 500
CD ₃ -Ala ₁₃	37700		58.2	212.3		6025 ± 500

CD ₃ -Ala ₁₅	37700	58.6	15.0	<i>500 ± 500</i>
CD ₃ -Ala ₁₇	37700	58.3	176.9	<i>6075 ± 500</i>

Table 2: Tensor components of the interactions used in the fitting procedure and experimental NMR parameters reflecting the peptide's dynamical behavior

* experimental static values measured on dry peptides, [†] computed values, [‡] (*italic*): dynamically averaged values (measured on membrane inserted peptide, at a weight % water of 33%). $CSA_{exp} = \delta_{90^\circ} - \delta_{iso} = 3/2 (\delta_{90^\circ} - \delta_{iso})$ for peptide in axial diffusion around the lipid bilayer normal. $\delta_{aniso} = \delta_{33} - \delta_{iso}$, $\eta = (\delta_{22} - \delta_{11}) / (\delta_{33} - \delta_{iso})$, with $|\delta_{33} - \delta_{iso}| \geq |\delta_{11} - \delta_{iso}| \geq |\delta_{22} - \delta_{iso}|$, $(\alpha_{PM}^i, \beta_{PM}^i, \gamma_{PM}^i)$ and (Theta, Phi) are the angles defining the CSA and dipolar or quadrupolar tensors orientation in the molecular frame (see Materials and Methods section). Experimental uncertainties were estimated from two independent experiments and several sets of fitting parameters. They were not sensitive to line width and the values finally retained and given in this table are very conservatives (10% relative error in most cases, 5% for ¹⁵N CSAs).

Number and nature of constraints		τ_0 (°)	$\Delta\tau$ (°)	ρ_0 (°)	$\Delta\rho$ (°)
		tilt	wobbling	rotation	oscillation
A	12: complete ensemble (SSD = 0.36)	20.8 ± 1.4	12.2 ± 4.5	146 ± 7	84 ± 21
B	10: remove ^{15}N - ^{13}C DC (SSD = 0.33)	21.0 ± 1.5	10.8 ± 6.3	146 ± 7	86 ± 19
C	14: adding 2 simulated ^{15}N -H DC [†]	20.4 ± 1.8	11.3 ± 7.3	146 ± 6	82 ± 23
D	6: 2 ^{15}N CSA, 2 ^{13}C CSA, 2 CD_3 $\Delta\nu_Q$	21.9 ± 1.3	8.0 ± 6.5	149 ± 8	90 ± 20
E	8: 6 CD_3 + 2 ^{15}N CSA	21.2 ± 1.8	11.5 ± 5.5	147 ± 7	83 ± 28
F1	6 : CD_3 $\Delta\nu_Q$ alone (sol a: SSD = 0.3)	2.8 ± 0.9	31.9 ± 1.7	147 ± 8	80 ± 21
F2	6 : CD_3 $\Delta\nu_Q$ alone (sol b: SSD = 0.6)	21.2 ± 1.0	1.3 ± 1.3	146 ± 8	75 ± 36
H	4: 2 ^{15}N CSA + 2 ^{15}N -H DC	15.8 ± 1.6	23.9 ± 2.0	127 ± 109	30 ± 81

Table 3: Best fit parameters using various subsets of anisotropic NMR constraints and uniform distributions

Every fits were performed using the data obtained at 33% hydration (water/(water+lipid+peptide), w/w). The fits presented in this table result from uniform distributions (see main text, comment ‘d’ for Gaussian distributions). The uncertainty of each parameter (3σ values) was computed by the Monte Carlo approach (36) as described in the “Materials and methods” section; [†] the simulated ^{15}N -H dipolar couplings have been computed using the dynamical parameters obtained from solution A. SSD is the standard deviation.

Figure Legends

Figure 1: Influence of dynamical averaging on quadrupolar splitting; a) Dynamic model describing the orientation and the dynamics of the peptide by a wobbling ($\Delta\tau$) in a cone around the averaged value of the helix tilt angle (τ_0) and an oscillations ($\Delta\rho$) around averaged value of helix rotation angle (ρ_0); the fast axial diffusion takes place around the bilayer normal; the three graphs represent the dependence of the quadrupolar splitting as a function of the label position around the helix (characterized by the ψ angle). b) variation for four tilt angles τ_0 (1° , 10° , 20° , 30°), no wobbling, no oscillation; c) variation for a tilt angle of $\tau_0 = 12^\circ$, oscillations $\Delta\rho = 1^\circ$; 20° ; 100° ; 150° ; d) comparison of three dynamical models: ($\tau_0 = 12^\circ$, $\Delta\tau = 0^\circ$, $\Delta\rho = 0^\circ$) ; ($\tau_0 = 6^\circ$, $\Delta\tau = 10^\circ$, $\Delta\rho = 0^\circ$); ($\tau_0 = 18^\circ$, $\Delta\tau = 0^\circ$, $\Delta\rho = 80^\circ$). All the plots were obtained for a same value of helix rotation angle (ρ_0).

Figure 2: Schematic representation of eigenvector orientation with respect to the peptide plane for $^{13}\text{C}_1$ and ^{15}N CSA tensors.

Figure 3: ^{13}C (a,c) and ^{15}N (b,d) MAS NMR spectra for CSA determination for WALP23[$^2\text{H}_3$ -Ala $_{13}$, $^{13}\text{C}_1$ -Ala $_{11}$, ^{15}N -Leu $_{12}$] peptide in DMPC liposomes (molar ratio 1:100, weight % water of 33%) (a,b) and as a dry peptide (c,d). (a) $^{13}\text{C}_1$ -Ala $_{11}$ spinning side band spectrum measured at 1 kHz spinning frequency. The peaks labeled with stars correspond to signal from lipid carbonyls. (b) Overlay of: (black) ^{15}N -Leu $_{12}$ 10 kHz spinning MAS NMR spectrum and (grey) ^{15}N -Leu $_{12}$ NMR powder spectrum of liposomes displaying the highest intensity for bilayers oriented at 90° . Similar data were obtained for WALP23[$^2\text{H}_3$ -Ala $_7$, $^{13}\text{C}_1$ -Ala $_{13}$, ^{15}N -Leu $_{14}$] peptide in DMPC liposomes (data not shown). (c) $^{13}\text{C}_1$ -Ala $_{11}$ spinning side band spectrum at 4 kHz spinning frequency, on dry peptide. (d) ^{15}N -Leu $_{12}$ spinning side band spectrum measured at 3 kHz spinning frequency on dry peptide. Similar data were obtained for WALP23[$^2\text{H}_3$ -Ala $_7$, $^{13}\text{C}_1$ -Ala $_{13}$, ^{15}N -Leu $_{14}$] peptide (data not shown).

Figure 4: Best fit (grey bars) to the 12 experimental anisotropic constraints obtained from NMR (light grey bars) corresponding to results on line A of Table 1: a) CD_3 quadrupolar couplings (in Hz) of Ala $_{7,9,11,13,15,17}$ (1 to 6 respectively); b) ^{15}N - $^{13}\text{C}_1$ dipolar couplings (in Hz) of Ala $_{11}$ -Leu $_{12}$ (1) and Ala $_{13}$ -Leu $_{14}$ (2); c) Chemical Shift Anisotropies of $^{13}\text{C}_1$ -Ala $_{11}$ (1) and Ala $_{13}$ (2) (in Hz) and ^{15}N -Leu $_{12}$ (3) and Leu $_{14}$ (4) (in Hz). The experimental values are summarized in Table 2.

Figure 1

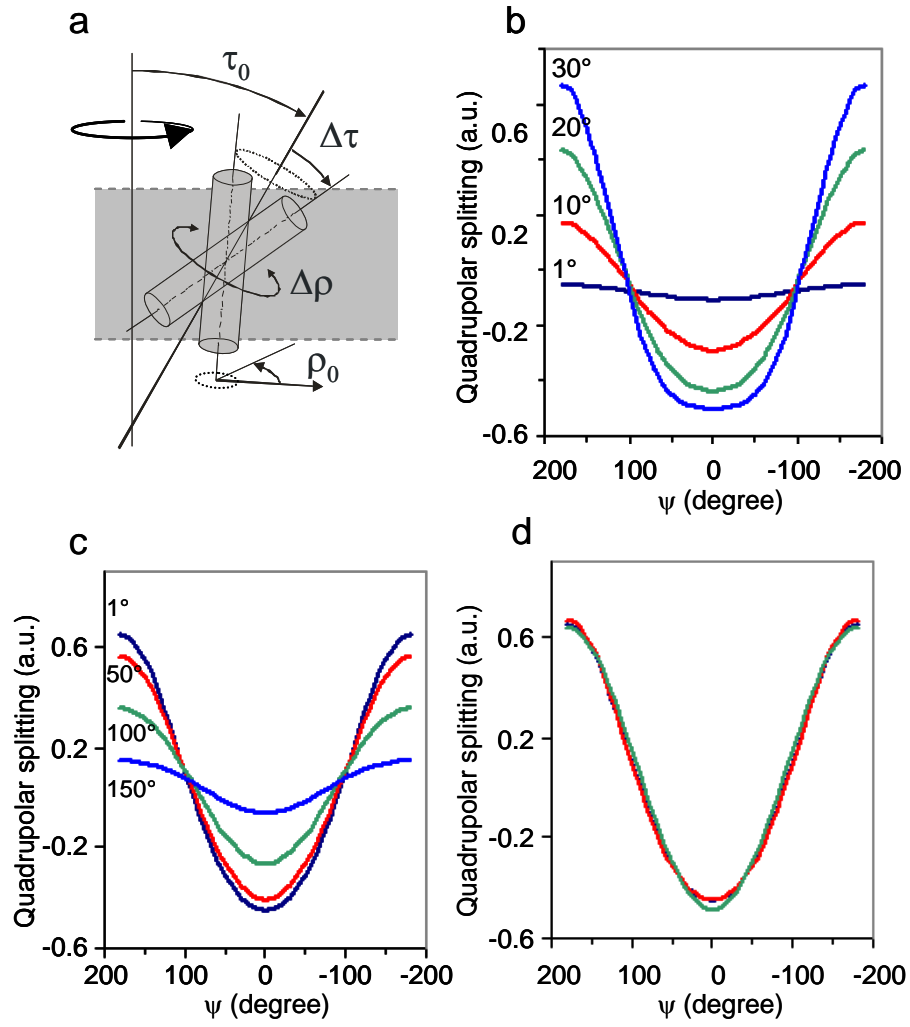


Figure 2

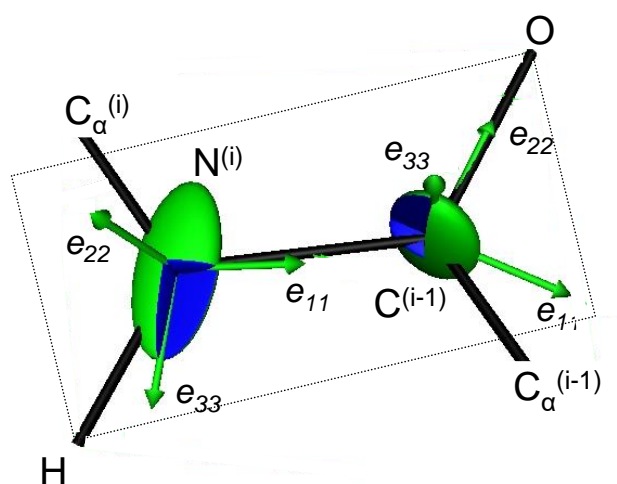


Figure 3

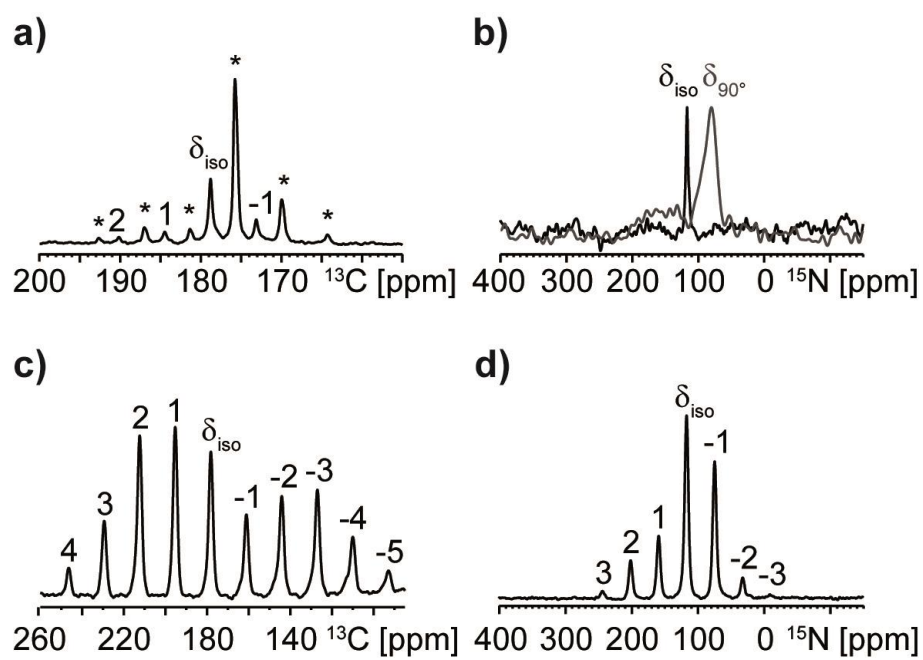
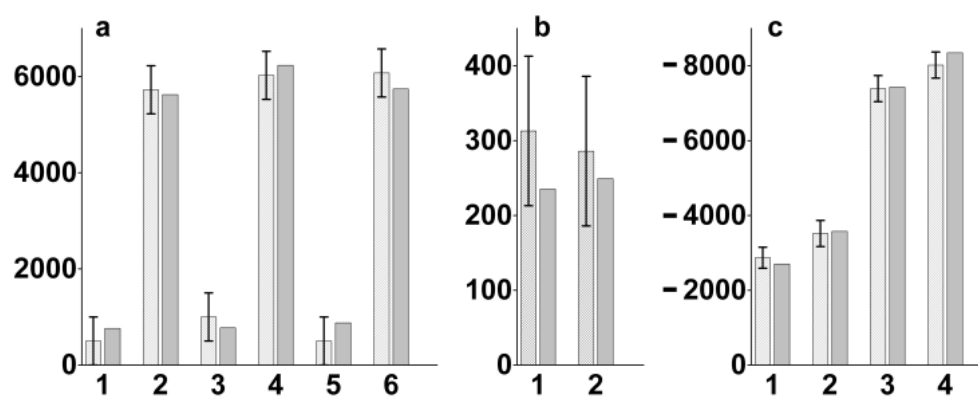


Figure 4



Supporting material

NMR data acquisition

Cross-polarization magic-angle spinning (CP-MAS) spectra were acquired using a ^1H excitation pulse length of 2 μs and a CP spin-lock field-strength of 50 kHz. The CP contact time was 2 ms and 1.25 ms for ^{13}C and ^{15}N spectra, respectively. The ^1H radio-frequency field-strength for heteronuclear two-pulse phase-modulation (TPPM) decoupling was 125 kHz during acquisition. The repetition delay was 2 s.

Static ^{13}C - ^{15}N dipolar couplings were determined using a standard REDOR (1) experiment at a spinning frequency of 10 kHz. The ^{15}N π pulse length was 9.9 μs and the pulses were phased according to the xy-4 scheme (2). The ^{13}C π pulse length was 8 μs . CW and TPPM ^1H decoupling at 125 kHz were applied during the evolution time and acquisition, respectively. The $\Delta\text{S}/\text{S}_0$ REDOR curves were fitted in a standard manner (3) using Mathcad software (4), with 13 mixing times ranging from 0 to 5 ms by 400 μs increments.

Deuterium $\pi/2$ pulses were equal to 3 μs and the refocusing delay and the repetition time were set to 10 s. *WALP23 in membrane*: Each peptide was reconstituted into bilayers of DMPC lipids at a 1:100 molar ratio and subjected to a series of NMR measurements at 313 K. Liposomes were used instead of oriented bilayers to allow complete control of the hydration level. The amount of proteoliposomes used in MAS NMR experiments was about 35 mg. Isotropic chemical shifts were determined under CP-MAS conditions at a spinning frequency of 10 kHz. CP-MAS spectra were acquired using a ^1H excitation pulse length of 2.9 μs and a CP spin-lock field-strength of 50 kHz. The CP contact time was 4.5 ms for ^{13}C and 1.5 ms for ^{15}N spectra. The ^1H radio-frequency field-strength for heteronuclear TPPM decoupling was 86 kHz during acquisition. The repetition delay was 3 s to avoid sample heating. ^{13}C - ^{15}N dipolar coupling was determined using a standard REDOR experiment at a spinning frequency of 10 kHz. The ^{15}N π pulse length was 10 μs and the pulses were phased according to the xy-4 scheme. The ^{13}C π pulse length was 10 μs . CW and TPPM ^1H decoupling at 86 kHz were applied during the evolution time and acquisition, respectively. Deuterium NMR spectra, i.e. quadrupolar interactions, of CD_3 Ala7 and Ala13 were acquired using the same procedure as for static measurements on dry peptide but with repetition time sets to 0.3 s. The four remaining quadrupolar interactions were extracted from the literature ⁽⁵⁾.

Angle definitions for computing anisotropic interactions:

Both quadrupolar and dipolar splittings were computed from the expression:

$$g(\beta_{PN}^{QC/DC}) = K_{QC/DC} \cdot \frac{3\cos^2 \beta_{PN}^{QC/DC} - 1}{2}$$

where the constant $K_{QC/DC}$ depends on the type of interaction, quadrupolar (QC) or dipolar coupling (DC), respectively. $\beta_{PN}^{QC/DC}$ defines the orientation of the bilayer normal \vec{N} relative to the principal axis frame of dipolar or quadrupolar interaction tensor (C-D quadrupolar tensor being quasi axially

symmetric). This equation is given for bilayers oriented with the bilayer normal parallel to the magnetic field.

The Chemical Shift Anisotropy (CSA) effects depend on the spherical coordinates β_{PN}^{CSA} and α_{PN}^{CSA} of the bilayer normal \vec{N} in the principal axis frame (PAF) of the CSA tensor (where η is the asymmetry parameter):

$$h(\beta_{PN}^{CSA}, \alpha_{PN}^{CSA}) = -K'_{CSA} \cdot \left[\left(\frac{3 \cos^2 \beta_{PN}^{CSA} - 1}{2} \right) + \frac{1}{2} \eta (\sin^2 \beta_{PN}^{CSA} \cos 2\alpha_{PN}^{CSA}) \right]$$

Following the Wigner rotation matrix formalism (6), equations $g(\beta_{PN}^{QC/DC})$ and $h(\beta_{PN}^{CSA}, \alpha_{PN}^{CSA})$ were expressed as function of the PAS orientation relative to the molecular frame (noted M) and M frame orientation relative to the diffusion frame (noted N), as describe in figure 1s.

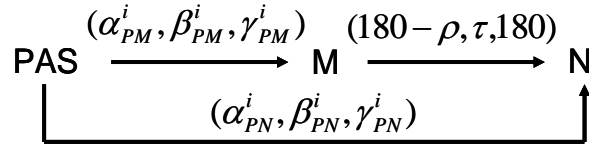


Figure 1s: Schematic representation of frame transformations and Euler angles definition.

$(\alpha_{PM}^i, \beta_{PM}^i, \gamma_{PM}^i)$ are the Euler angles associated to the rotation matrix between the tensor principal axis system PASⁱ and the molecular frame M. For quadrupolar and dipolar interactions $\beta_{PM}^{QC/DC}$ and $(180 - \gamma_{PM}^{QC/DC})$ represent the spherical coordinates of the axially symmetric tensor in frame M and $\alpha_{PM}^{QC/DC}$ is set to zero. $(180 - \rho, \tau, 180)$ are the Euler angles associated to the rotation matrix between the molecular frame M and the diffusion frame N. $(\alpha_{PN}^i, \beta_{PN}^i, \gamma_{PN}^i)$ are the Euler angles corresponding to the rotation from PASⁱ to N. For the quadrupolar and dipolar interaction $\alpha_{PN}^{QC,DC}$ and $\gamma_{PN}^{QC/DC}$ are equal to zero due to the axial symmetry of both the PAS and the N frames. For the chemical shift anisotropy interaction, only γ_{PN}^{CSA} is set to zero. With GALA (7, 8) the angle definitions are $\beta_{PM}^{QC} = \varepsilon_{||}$, $\gamma_{PM}^{QC} = \delta = \psi + \rho$, where ψ is geometry-dependent, ρ is the helix rotation angle and $(-\rho, -\tau)$ are the polar coordinates of diffusion axis \vec{N} (bilayer normal) in the molecular frame M.

Dynamical averaging of the anisotropic interactions:

Peptide motion in the sub-microsecond time scale leads to time-modulated β_{PN}^i and α_{PN}^i angles, and was included by integrating $g(\beta_{PN}^{QC/DC})$ and $h(\beta_{PN}^{CSA}, \alpha_{PN}^{CSA})$ over the angles describing the movements i.e. variation of τ between $\tau_0 - \Delta\tau$ and $\tau_0 + \Delta\tau$ and of ρ between $\rho_0 - \Delta\rho$ and $\rho_0 + \Delta\rho$, according to the following equations.

$$\langle f(\beta_{PN}^i, \alpha_{PN}^i) \rangle = \frac{\int_0^{2\pi} \int_0^{\Delta\tau} \int_{-\Delta\rho}^{\Delta\rho} f(\beta_{PN}^i, \alpha_{PN}^i) \sin \tau_1 d\rho_1 d\tau_1 d\phi}{\int_0^{2\pi} \int_0^{\Delta\tau} \int_{-\Delta\rho}^{\Delta\rho} \sin \tau_1 d\rho_1 d\tau_1 d\phi}$$

for a uniform distribution, and:

$$\langle f(\beta_{PN}^i, \alpha_{PN}^i) \rangle = \frac{\int_0^{2\pi} \int_0^{3(\Delta\tau)} \int_{-3(\Delta\rho)}^{3(\Delta\rho)} f(\beta_{PN}^i, \alpha_{PN}^i) \sin \tau_1 \exp\left(-\frac{\tau_1^2}{2(\Delta\tau)^2}\right) \cdot \exp\left(-\frac{\rho_1^2}{2(\Delta\rho)^2}\right) d\rho_1 d\tau_1 d\phi}{\int_0^{2\pi} \int_0^{3(\Delta\tau)} \int_{-3(\Delta\rho)}^{3(\Delta\rho)} \sin \tau_1 \exp\left(-\frac{\tau_1^2}{2(\Delta\tau)^2}\right) \cdot \exp\left(-\frac{\rho_1^2}{2(\Delta\rho)^2}\right) d\rho_1 d\tau_1 d\phi}$$

for a Gaussian distribution.

With $f(\beta_{PN}^i, \alpha_{PN}^i) = g(\beta_{PN}^{QC/DC})$, $\alpha_{PN}^{QC,DCi} = 0$ for quadrupolar and dipolar interactions, and

$h(\beta_{PN}^{CSA}, \alpha_{PN}^{CSA})$ for chemical shift anisotropic interaction

Figure 2s describes the various motion considered and defines the integration variables.

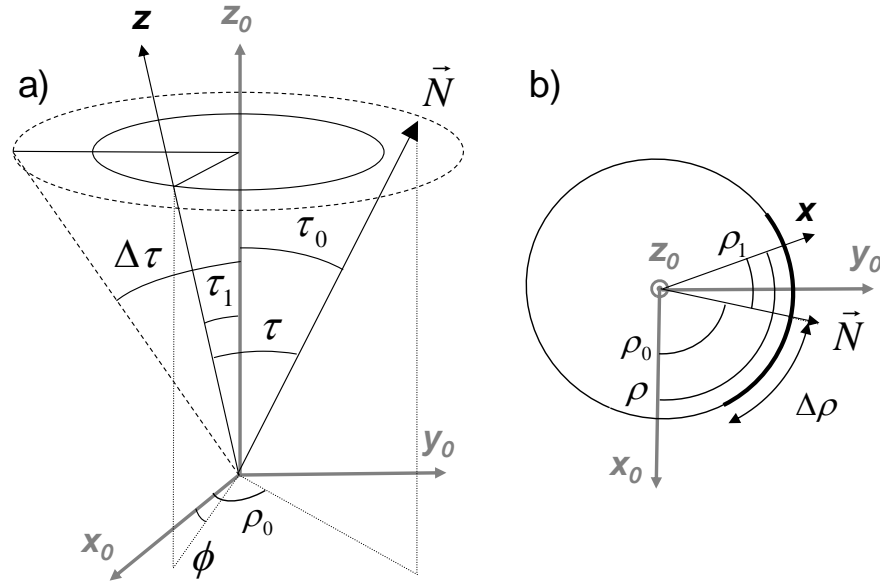


Figure 2s: schematic representation of integrating variables: a) 3D representation of the various frames and vectors involved b) 2D projection in the (x,y) plane of the molecular frame.

\vec{N} is the bilayer normal and main diffusion axis. (x_0, y_0, z_0) represents the molecular frame at its average position (for which τ_0 and ρ_0 defines the position of \vec{N}). (z) represents the molecular frame z axis (i.e. the main helix inertia axis) at a certain time. z is wobbling around its average position z_0 in a cone of angle $\Delta\tau$ (integration over τ_1 varying between 0 and $\Delta\tau$, and over ϕ varying between 0 and 2π). The 2D projection in the (x_0, y_0) plane defines the helix oscillation: the rotation angle ρ fluctuates around its average value ρ_0 , with an amplitude $\Delta\rho$ (integration over ρ_1 varying between $-\Delta\rho$ and $+\Delta\rho$). In the case of Gaussian distributions the integration was performed over $3\Delta\tau$ and $3\Delta\rho$ i.e. over 3 times the distribution's standard deviations. The instantaneous tilt angle τ and rotation angle ρ are linked to the other variables by the equations $\rho = \rho_0 + \rho_1$ and $\cos \tau = \cos \tau_0 \cdot \cos \tau_1 - \sin \tau_0 \cdot \sin \tau_1 \cdot \cos \phi$

Reference:

1. Gullion, T., and J. Schaefer. 1989. Rotational-Echo Double-Resonance NMR. *J. Magn. Reson.* 81:196-200.
2. Gullion, T., D. B. Baker, and M. S. Conradi. 1990. New, Compensated Carr-Purcell Sequences. *J. Magn. Reson.* 89:479-484.
3. Gullion, T., and J. Schaefer. 1989. Rotational-Echo Double-Resonance NMR. *Adv. Magn. Reson.* 13:57.
4. Mathcad. 1986-2000. *MathSoft, Inc.*
5. Strandberg, E., S. Ozdirekcan, D. T. S. Rijkers, P. C. A. van der Wel, R. E. Koeppe, R. M. J. Liskamp, and J. A. Killian. 2004. Tilt angles of transmembrane model peptides in oriented and non-oriented lipid bilayers as determined by H-2 solid-state NMR. *Biophys. J.* 86:3709-3721.
6. Schmidt-Rohr, K., and H. W. Spiess. 1994. In *Multidimensional solid-state NMR and polymers*. A. Press, editor. Harcourt Brace & Company, London. 444-452.
7. Ozdirekcan, S., D. T. S. Rijkers, R. M. J. Liskamp, and J. A. Killian. 2005. Influence of flanking residues on tilt and rotation angles of transmembrane peptides in lipid bilayers. A solid-state H-2 NMR study. *Biochemistry* 44:1004-1012.
8. van der Wel, P. C. A., E. Strandberg, J. A. Killian, and R. E. Koeppe. 2002. Geometry and intrinsic tilt of a tryptophan-anchored transmembrane alpha-helix determined by H-2 NMR. *Biophys. J.* 83:1479-1488.